

# CHEMISTRY OF MATERIALS

VOLUME 19, NUMBER 8

APRIL 17, 2007

© Copyright 2007 by the American Chemical Society

## Communications

### Ambient-Pressure Synthesis of SHG-Active $\text{Eu}_2\text{Ti}_2\text{O}_7$ with a [110] Layered Perovskite Structure: Suppressing Pyrochlore Formation by Oxidation of Perovskite-Type $\text{EuTiO}_3$

Nathaniel L. Henderson,<sup>†</sup> Jaewook Baek,<sup>‡</sup>  
P. Shiv Halasyamani,<sup>\*,‡</sup> and Raymond E. Schaak<sup>\*,†</sup>

Department of Chemistry, Texas A&M University,  
College Station, Texas 77842, and Department of Chemistry,  
University of Houston, Houston, Texas 77204

Received December 11, 2006

Revised Manuscript Received February 23, 2007

Layered perovskites of formula  $A_2B_2O_7$  ( $A$  = alkaline earth or rare earth metal;  $B$  = transition metal), which are derived from the  $ABO_3$  perovskite structure by separating layers of corner-sharing  $BO_6$  octahedra along the [110] plane,<sup>1</sup> are important materials with a range of useful physical properties, including ferroelectricity,<sup>2</sup> second harmonic generation (SHG),<sup>3</sup> and photocatalytic activity for water splitting.<sup>4,5</sup> Common examples of [110] layered perovskites include  $\text{La}_2\text{Ti}_2\text{O}_7$ ,  $\text{Sr}_2\text{Nb}_2\text{O}_7$ , and  $\text{Ca}_2\text{Nb}_2\text{O}_7$ .<sup>6–8</sup> An alternative  $A_2B_2O_7$  structure is pyrochlore, which tends to be stabilized by smaller  $A$ -site

cations.<sup>9</sup> For example,  $\text{La}_2\text{Ti}_2\text{O}_7$  and  $\text{Nd}_2\text{Ti}_2\text{O}_7$  are [110] layered perovskites, whereas  $\text{Sm}_2\text{Ti}_2\text{O}_7$ ,  $\text{Eu}_2\text{Ti}_2\text{O}_7$ ,  $\text{Lu}_2\text{Ti}_2\text{O}_7$ , and  $\text{Y}_2\text{Ti}_2\text{O}_7$  are pyrochlores. For the smaller rare earth titanates such as  $\text{Eu}_2\text{Ti}_2\text{O}_7$ , the pyrochlore structure dominates.<sup>9</sup> Accordingly, the [110] layered perovskite modification of  $\text{Eu}_2\text{Ti}_2\text{O}_7$  has been accessed only using high-pressure (> 3 GPa) techniques.<sup>10,11</sup>

Here, we report a new low-temperature ambient-pressure strategy for synthesizing gram-scale quantities of the high-pressure [110] layered perovskite modification of  $\text{Eu}_2\text{Ti}_2\text{O}_7$ . The synthetic process is highlighted in Figure 1a. The approach utilizes  $\text{EuTiO}_3$ , a well-known simple cubic perovskite,<sup>12</sup> as a structural solid-state precursor. Upon heating in air or  $\text{O}_2$ , the  $\text{Eu}^{2+}$  in  $\text{EuTiO}_3$  oxidizes to  $\text{Eu}^{3+}$  and oxygen intercalates into the structure. The product,  $\text{Eu}_2\text{Ti}_2\text{O}_7$ , retains the perovskite motif defined by the  $\text{EuTiO}_3$  precursor and allows the [110] layered perovskite polymorph of  $\text{Eu}_2\text{Ti}_2\text{O}_7$  to crystallize before the more stable pyrochlore structure forms. Thus, by utilizing  $\text{EuTiO}_3$  as a precursor, the formation of pyrochlore-type  $\text{Eu}_2\text{Ti}_2\text{O}_7$  is suppressed, providing a narrow temperature window in which the [110] layered perovskite structure is stable at ambient pressure.

The  $\text{EuTiO}_3$  precursor was synthesized by heating stoichiometric amounts of  $\text{Eu}_2\text{O}_3$  and  $\text{TiO}_2$  for 24 h at 1000 °C under flowing  $\text{H}_2/\text{Ar}$  (5%/95%). ( $\text{EuTiO}_3$  can also be synthesized by reducing pyrochlore-type  $\text{Eu}_2\text{Ti}_2\text{O}_7$  in  $\text{H}_2/\text{Ar}$

\* To whom correspondence should be addressed. E-mail: psh@uh.edu (P.S.H.); schaak@mail.chem.tamu.edu (R.E.S.).

<sup>†</sup> Texas A&M University.

<sup>‡</sup> University of Houston.

- (1) Lichtenberg, F.; Herrnberger, A.; Wiedenmann, K.; Mannhart, J. *Prog. Solid State Chem.* **2001**, 29, 1.
- (2) Sandstrom, M. M.; Fuierer, P. J. *Mater. Res.* **2003**, 18, 357.
- (3) Zakharov, N. A.; Krikorov, V. S.; Kustov, E. F.; Stefanovich, S. Y. *Phys. Status Solidi* **1978**, 50, K13.
- (4) Kim, J.; Hwang, D. W.; Kim, H.-G.; Bae, S. M.; Ji, S. M.; Lee, J. S. *Chem. Commun.* **2002**, 2488.
- (5) Hwang, D. W.; Lee, J. S.; Li, W.; Oh, S. H. *J. Phys. Chem. B* **2003**, 107, 4963.
- (6) Gasperin, P. M. *Acta Crystallogr., Sect. B* **1975**, 31, 2129.
- (7) Schmalte, H. W.; Williams, T.; Reller, A.; Linden, A.; Bednorz, J. G. *Acta Crystallogr., Sect. B* **1993**, 49, 235.

- (8) Ishizawa, N.; Marumo, F.; Iwai, S.; Kimura, M.; Kawamura, T. *Acta Crystallogr., Sect. B* **1980**, 36, 763.
- (9) Subramanian, M. A.; Aravamudan, G.; Subba Rao, G. V. *Prog. Solid State Chem.* **1983**, 15, 55.
- (10) Bondarenko, T. N.; Uvarov, V. N.; Borisenko, S. V.; Teterin, Y. A.; Dzeganzovskii, V. P.; Sych, A. M.; Titiv, Y. A. *J. Korean Phys. Soc.* **1998**, 32, S65.
- (11) Sych, A. M.; Stefanovich, S. Y.; Titov, Y. A.; Bondarenko, T. N.; Mel'nik, V. M. *Inorg. Mater.* **1991**, 27, 2229.
- (12) McCarthy, G. J.; White, W. B.; Roy, R. *Mater. Res. Bull.* **1969**, 4, 251.

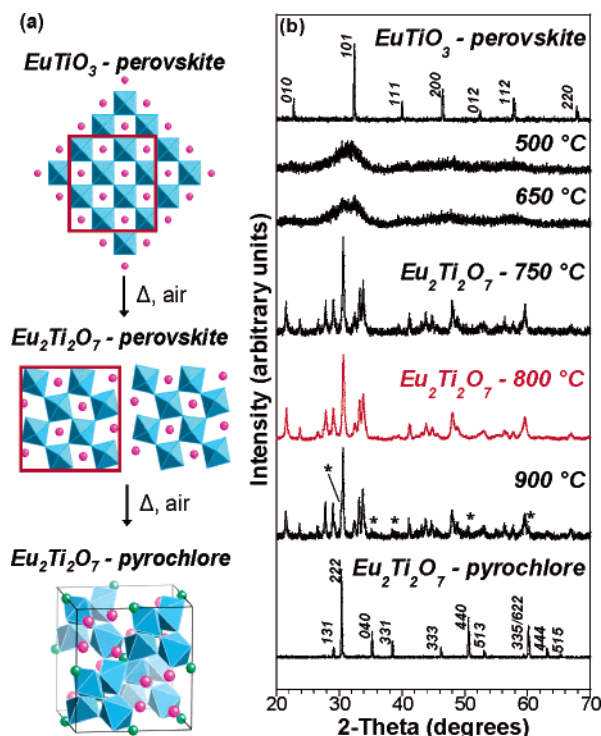


**Figure 1.** (a) Overview of the ambient-pressure synthetic pathway used to access  $\text{Eu}_2\text{Ti}_2\text{O}_7$  with a [110] layered perovskite structure. The simple perovskite  $\text{EuTiO}_3$  is thermally oxidized to form perovskite-type  $\text{Eu}_2\text{Ti}_2\text{O}_7$ , which then transforms to pyrochlore-type  $\text{Eu}_2\text{Ti}_2\text{O}_7$  with continued heating. The light blue polyhedra represent  $\text{TiO}_6$  octahedra, and the pink spheres represent Eu cations. In the pyrochlore structure, oxygen atoms that are not part of the  $\text{TiO}_6$  octahedra are shown as green spheres. (b) Powder XRD data for the  $\text{EuTiO}_3$  precursor, the amorphous perovskite-related intermediate (500 and 650 °C), the crystallization of perovskite-type  $\text{Eu}_2\text{Ti}_2\text{O}_7$  (750, 800, and 900 °C), and the stable  $\text{Eu}_2\text{Ti}_2\text{O}_7$  pyrochlore phase that forms at higher temperatures. The pattern highlighted in red (800 °C) is phase-pure perovskite-type  $\text{Eu}_2\text{Ti}_2\text{O}_7$  (as determined by laboratory XRD). The asterisks in the 900 °C XRD pattern show the presence of some pyrochlore-type  $\text{Eu}_2\text{Ti}_2\text{O}_7$ .

at 1000 °C.) The X-ray diffraction (XRD) pattern for the black  $\text{EuTiO}_3$  powder (Figure 1b) matches that expected for the simple perovskite. When  $\text{EuTiO}_3$  is heated in air, it initially forms an amorphous perovskite-related intermediate (Figure 1b) that is present between 475 and 650 °C. At 750 °C, the [110] layered perovskite polymorph of  $\text{Eu}_2\text{Ti}_2\text{O}_7$  begins to crystallize, and it is stable up to 800 °C. By 900 °C, impurities of pyrochlore-type  $\text{Eu}_2\text{Ti}_2\text{O}_7$  are evident by XRD, and the sample converts entirely to the pyrochlore polymorph above 1000 °C (Figure 1b). In a typical large-scale synthesis of phase-pure perovskite-type  $\text{Eu}_2\text{Ti}_2\text{O}_7$ , a 2 g batch of  $\text{EuTiO}_3$  is heated to 800 °C in air for 15 h (Figure 1b).

The XRD pattern for  $\text{Eu}_2\text{Ti}_2\text{O}_7$  synthesized by oxidation of  $\text{EuTiO}_3$  matches that of  $\text{La}_2\text{Ti}_2\text{O}_7$ , which suggests that the two compounds are isostructural.  $\text{La}_2\text{Ti}_2\text{O}_7$  crystallizes in the monoclinic space group  $P2_1$  at room temperature.<sup>6</sup> However,  $\text{La}_2\text{Ti}_2\text{O}_7$  can also adopt an orthorhombic ( $Pna2_1$ ) modification through twinning and stacking of two monoclinic cells.<sup>7</sup> The differences between these two structures, and therefore the differences in their powder XRD patterns, are subtle. On the basis of a few weak reflections in the powder XRD data (see the Supporting Information) and by analogy to the room-temperature structure of  $\text{La}_2\text{Ti}_2\text{O}_7$ , we propose that perovskite-type  $\text{Eu}_2\text{Ti}_2\text{O}_7$  also adopts the  $P2_1$

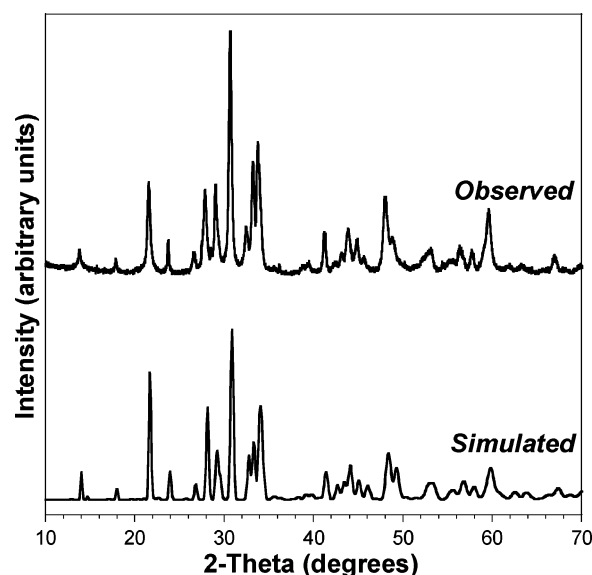


**Figure 2.** Observed and simulated diffraction patterns for  $\text{Eu}_2\text{Ti}_2\text{O}_7$  with a [110] layered perovskite structure. The simulated XRD pattern was calculated using atomic coordinates for monoclinic  $\text{La}_2\text{Ti}_2\text{O}_7$  (ref 6) and refined lattice constants for  $\text{Eu}_2\text{Ti}_2\text{O}_7$ .

monoclinic structure of  $\text{La}_2\text{Ti}_2\text{O}_7$ . However, the broad peaks observed in the powder XRD pattern of perovskite-type  $\text{Eu}_2\text{Ti}_2\text{O}_7$  (likely the result of limited crystallinity because of the relatively low temperatures necessary to access it), as well as a non-negligible background (likely originating from some residual amorphous intermediate), make structure refinement difficult (see the Supporting Information). Assuming a monoclinic structure analogous to that of  $\text{La}_2\text{Ti}_2\text{O}_7$ , the refined unit-cell parameters for perovskite-type  $\text{Eu}_2\text{Ti}_2\text{O}_7$  are  $a = 7.54(1)$  Å,  $b = 5.391(8)$  Å,  $c = 12.91(3)$  Å, and  $\beta = 98.3(9)^\circ$ . The unit-cell volume of monoclinic  $\text{Eu}_2\text{Ti}_2\text{O}_7$  is 520.0 Å<sup>3</sup>, which is smaller than that of monoclinic  $\text{La}_2\text{Ti}_2\text{O}_7$  (557.0 Å<sup>3</sup>),<sup>7</sup> as expected. The good agreement between the observed XRD data for perovskite-type  $\text{Eu}_2\text{Ti}_2\text{O}_7$  and the simulated data using the structure of monoclinic  $\text{La}_2\text{Ti}_2\text{O}_7$  as a model (Figure 2) is consistent with this proposed structural assignment. (See the Supporting Information for a more detailed comparison between the simulated and experimental XRD data.)

Because perovskite-type  $\text{La}_2\text{Ti}_2\text{O}_7$  is known to be ferroelectric and SHG-active,<sup>3</sup> we measured these properties for perovskite-type  $\text{Eu}_2\text{Ti}_2\text{O}_7$  synthesized by oxidizing  $\text{EuTiO}_3$  at 800 °C for 15 h. Powder SHG measurements on polycrystalline  $\text{Eu}_2\text{Ti}_2\text{O}_7$  were performed on a modified Kurtz–NLO system using 1064 nm radiation.<sup>13</sup> A detailed description of the equipment and the methodology used has been published.<sup>14,15</sup> No index-matching fluid was used in any of the experiments. Powders with particle sizes of 45–63 μm were used for comparing SHG intensities. Ferroelectric measurements were performed on pressed sintered pellets 1/2 in. in diameter and ~1 mm thick. A detailed description

(13) Kurtz, S. K.; Perry, T. T. *J. Appl. Phys.* **1968**, 39, 3798–3813.

(14) Ok, K. M.; Bhuvanesh, N. S. P.; Halasyamani, P. S. *Inorg. Chem.* **2001**, 40, 1978–1980.

(15) Porter, Y.; Ok, K. M.; Bhuvanesh, N. S. P.; Halasyamani, P. S. *Chem. Mater.* **2001**, 13, 1910–1915.

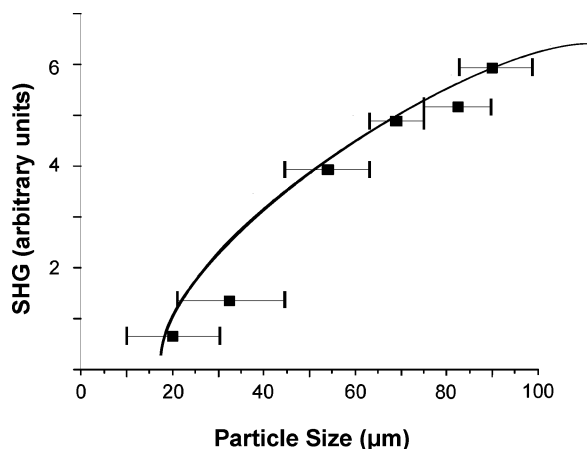


**Figure 3.** SHG efficiencies for various particle sizes of perovskite-type  $\text{Eu}_2\text{Ti}_2\text{O}_7$ , which is type 1 phase-matchable with an efficiency of  $80 \times \alpha\text{-SiO}_2$ . The curve is drawn as a guide to the eye rather than as a fit to the data.

of the instrument and technique has been published.<sup>16</sup>  $\text{Eu}_2\text{Ti}_2\text{O}_7$  is not ferroelectric — no hysteresis loop was observed (see the Supporting Information). The small “gap” in the polarization vs voltage curve may be attributed to “leakage” in the material.

The powder SHG measurements indicate that perovskite-type  $\text{Eu}_2\text{Ti}_2\text{O}_7$  exhibits an SHG efficiency of approximately  $80 \times \alpha\text{-SiO}_2$  (Figure 3), placing the material in Class B as defined by Kurtz and Perry.<sup>13</sup> The efficiency results in a  $\langle d_{\text{eff}} \rangle$  of approximately 10.3 pm/V. Phase-matching experiments, i.e., particle size vs SHG efficiency, indicate the material is Type 1 phase-matchable. The magnitude of the SHG efficiency is dependent on both the magnitude and direction of the intra-octahedral distortion of the  $\text{Ti}^{4+}$  cations. Each  $\text{Ti}^{4+}$  cation is displaced from the center of its oxide octahedron, resulting in a local dipole moment, attributable to second-order Jahn–Teller effects.<sup>17–23</sup> To better quantify the magnitude and direction of these displacements, we used the SHAPE program.<sup>24</sup> The  $\text{Ti}^{4+}$  cations are displaced from the center of their oxide octahedron by 0.0392 Å for Ti(1); 0.0492 Å, Ti(2); 0.0674 Å, Ti(3); and 0.0752 Å, Ti(4) (see the Supporting Information). These magnitudes are well within the range reported earlier for oxides with octahedrally coordinated  $\text{Ti}^{4+}$  cations.<sup>25</sup> With respect to the direction of

the distortion, all of the  $\text{Ti}^{4+}$  cations are displaced toward a vertex (Ti(1) is slightly displaced off-vertex). Although the direction of the local displacements is similar, the distortions do not fully “constructively add”. Each  $\text{Ti}^{4+}$  cation displaces locally toward a vertex along the crystallographic [101] and  $[\bar{1}01]$  directions, resulting in a net moment along the [100] direction. Thus, there is some cancellation of the dipole moments. It is this cancellation that is thought to reduce the SHG efficiency.

Despite this, layered perovskite-type  $\text{Eu}_2\text{Ti}_2\text{O}_7$  shows a remarkable (8-fold) increase in SHG conversion efficiency relative to the lanthanum-containing analog, which possesses a conversion efficiency of  $10 \times \alpha\text{-SiO}_2$ .<sup>3</sup> Interestingly, we find that  $\text{Eu}_2\text{Ti}_2\text{O}_7$  synthesized by thermal oxidation of  $\text{EuTiO}_3$  has an increased optical response relative to perovskite-type  $\text{Eu}_2\text{Ti}_2\text{O}_7$  synthesized at high pressures, which was reported to have a conversion efficiency of roughly one-fourth that of  $\text{La}_2\text{Ti}_2\text{O}_7$ .<sup>11</sup> This difference is likely attributable to details in the SHG measurements. Previous studies reported SHG measurements on  $\sim 2 \mu\text{m}$  particles.<sup>11</sup> Because SHG intensities decrease dramatically with decreasing particle sizes (see Figure 3, for example), the higher optical response that we observe is likely a result of better optimized SHG measurements for larger particle sizes.

In summary, we have succeeded in synthesizing gram-scale quantities of the SHG-active [110] layered perovskite polymorph of  $\text{Eu}_2\text{Ti}_2\text{O}_7$ , which was previously only accessible using high-pressure techniques. The use of  $\text{EuTiO}_3$  as a structural precursor likely facilitates the stabilization of the perovskite polymorph at ambient pressure and at temperatures lower than the pyrochlore structure forms. This synthetic strategy may turn out to be applicable to other Eu-containing  $d^0$  oxides, possibly facilitating the formation of several other [110] perovskite phases that normally crystallize in the pyrochlore structure. Also, given the significant interest in  $\text{La}_2\text{Ti}_2\text{O}_7$  for optical,<sup>3</sup> electronic,<sup>2</sup> and photocatalytic applications,<sup>4,5</sup> perovskite-type  $\text{Eu}_2\text{Ti}_2\text{O}_7$  and related phases may also be prudent targets for further study.

**Acknowledgment.** The work at Texas A&M was supported by the U.S. Department of Energy (DE-FG02-06ER46333), the Robert A. Welch Foundation (Grant A-1583), and the Texas Advanced Research Program (Grant 010366-0002-2006). R.E.S. also acknowledges support from the Arnold and Mabel Beckman Foundation (Young Investigator Award) and DuPont (Young Professor Grant). We acknowledge Nattamai Bhuvanesh for his assistance with structure refinement. J.B. and P.S.H. thank the Robert A. Welch Foundation, the NSF-Career Program (DMR-0092054), and the NSF—Chemical Bonding Center (KK5110) for support. We also acknowledge David Casanova Cases (University of Barcelona) for assistance with the SHAPE program.

**Supporting Information Available:** Synthesis and characterization details for perovskite-type  $\text{Eu}_2\text{Ti}_2\text{O}_7$ . This material is available free of charge via the Internet at <http://pubs.acs.org>.

CM062934D

- (16) Ok, K. M.; Chi, E. O.; Halasyamani, P. S. *Chem. Soc. Rev.* **2006**, 35, 710.
- (17) Opik, U.; Pryce, M. H. L. *Proc. R. Soc. (London)* **1957**, A238, 425–447.
- (18) Bader, R. F. W. *Mol. Phys.* **1960**, 3, 137–151.
- (19) Bader, R. F. W. *Can. J. Chem.* **1962**, 40, 1164–1175.
- (20) Pearson, R. G. *J. Am. Chem. Soc.* **1969**, 91, 4947–4955.
- (21) Pearson, R. G. *J. Mol. Struct. (Theorchem)* **1983**, 103, 25–34.
- (22) Wheeler, R. A.; Whangbo, M.-H.; Hughbanks, T.; Hoffmann, R.; Burdett, J. K.; Albright, T. A. *J. Am. Chem. Soc.* **1986**, 108, 2222–2236.
- (23) Kunz, M.; Brown, I. D. *J. Solid State Chem.* **1995**, 115, 395–406.
- (24) Llunell, M.; Casanova, D.; Cirera, J.; Bofill, J. M.; Alemany, P.; Alvarez, S.; Pinsky, M.; Avnir, D. *SHAPE*, 1.1b ed.; University of Barcelona: Barcelona, Spain, 2004.
- (25) Ok, K. M.; Halasyamani, P. S.; Casanova, D.; Llunell, M.; Alemany, P.; Alvarez, S. *Chem. Mater.* **2006**, 18, 3176.